

PEV'S SMART CHARGING STRATEGY BASED ON INDIVIDUAL STATE OF CHARGE

Frederico Haasis^{1,2}, Oscar Solano², Bruno França¹, Daniel Dias¹

¹Federal Fluminense University, Niterói – RJ, Brazil

²Electrical Energy Research Center, Rio de Janeiro – RJ, Brazil

e-mail: fredaugusto18@gmail.com, oscar@cepel.br, bwfranca@id.uff.br, dhndias@id.uff.br

Abstract – The main contribution of this work is a smart-charging strategy based on the state of charge analyses to avoid the undervoltages caused by plug-in electric vehicles into the distribution system. The work uses power hardware-in-the-loop simulations, where a modified IEEE 34 bus system, with five groups of electric vehicle stations, is modeled in a real-time digital simulator. The number of electric vehicles charging and the initial state of charge (SoC) are generated randomly. The first analyses identify the undervoltage problems due to the increased number of electric vehicles connected during peak hours load. After, a smart-charging solution is necessary to solve this power quality problem. So, if the voltage profile decreases under certain limits, defined by a hysteresis band, the control occurs, and the smart-charging is applied. The proposed strategy based on individual state of charge priority reduces the electric vehicle recharge power at virtual stations, by comparing its value with the mean of state of charge values from each station group. The experimental results presented show that, by varying the recharge current, the voltage profiles do not reach the limit for sags determined by the Brazilian standard, proving the performance and solving the problem even if not reducing the recharge current of all electric vehicles equally.

Keywords – Plug-in Electric Vehicles, Power Hardware-in-the-loop, Power Quality, State-of-Charge, Smart-Charging, Undervoltage.

NOMENCLATURE

<i>PEVs</i>	Plug-in electric vehicles.
<i>SoC</i>	State of charge.
<i>PCC</i>	Point of common coupling.
<i>PHIL</i>	Power hardware in-the-loop.
<i>PA</i>	Power amplifier.
<i>RTS</i>	Real-time simulator.
<i>SC</i>	Smart-charging.
V_{rc}	Grid voltage connection.
I_{rc}	Nominal recharge current.
P_{rc}	Recharge power.

Manuscript received 06/29/2023; first revision 08/11/2023; accepted for publication 10/19/2023, by recommendation of Associate Editor Carlos Illa Font. <http://dx.doi.org/10.18618/REP.2023.4.0009>.



I. INTRODUCTION

Electric vehicles (EVs) could substantially reduce pollution levels in the mobility sector. The annual report from International Energy Agency (IEA) shows the world perspective and the evolution of EVs number in 2022, which surpassed the 10 million sales mark [1]. However, the number of charging stations is expanding at a different rate. Data available in this same report from IEA indicates the number of EVs per charging point around the world, where Brazil currently has around 32 EVs per charging station.

Even though this indicates how young the Brazilian market is and the necessity of pursuing more charging stations to meet the future demand from the EVs market, data from the Brazilian Association of Electric Vehicles (ABVE) indicates an increase of 58% (32,239) in the EVs market in the first semester of 2023 when compared to the same semester in 2022 (20,427 units), reaching the mark of 158,678 EV [2]. The market analysis includes Hybrids (HEV) and Plug-in Electric Vehicles (PEVs), which denote hybrids and fully electric cars.

The electrical system must support all the new connections for PEVs recharging, consequently demanding more energy from the grid. Grid operators have already monitored this intense connection focused on avoiding overload problems and power quality (PQ) issues [3], [4]. In this context, many studies have presented strategies for the better geographic location of charging stations and models of smart charging (SC) strategies [5]–[7].

The main worry about power quality occurs during peak load hours when PEVs connection to the grid could cause problems like undervoltage due to overload conditions. This problem can appear on the connection buses of the stations or other buses on the same grid.

Other technical studies have focused on how the charging station of EVs will influence the distribution system network. The work [8] presented the existing technologies to charge EVs and their strategies. Also [9] studied the behavior of EV users and their charging profiles to choose the best charging mode. In [10] they addressed the impacts of EVs charging at the grid by proposing intelligent charging solutions based on hierarchical control and comparing the benefits of this strategy. Also, the review work from [11] brought up the different types of voltage-based control inside the charging station, how they work when undervoltage occurs, their limitations, and the advantages of using centralized, decentralized, or autonomous control. Even though most studies presented in [11] treat every PEV connected to the grid with the same logic, this could be seen as unfair because each vehicle has a different battery state of charge (SoC). Therefore, PEVs with a lower SoC, when

compared to those with a higher SoC, have more possibilities to stay recharging for a longer time even when the first in first out (FIFO) strategy is applied.

Related to real-time testing strategies, Hardware-in-the-loop (HIL) and Power Hardware-in-the-loop (PHIL) have been used as important solutions to test equipment (Hardware or Software), in controllable conditions, before installing them into the operation field. Work [12] demonstrates how real-time tests can be used to diagnose the effects of large-scale EV integration into the electrical system. Also, [13] executed a real-time test to validate an energy management system for a fuel-cell hybrid electric vehicle. Furthermore, to connect the virtual grid to the actual component, some studies present possible configurations of power amplifiers (PA) with the RTS, called an interface algorithm (IA) [14].

Therefore, to contribute to the smart-charging (SC) field, this paper uses a PHIL setup to reveal the impact of uncontrolled PEVs charging into a simulated distribution benchmark grid, based on EV charging mode 3, as presented in Section II. Additionally, this work analyses and validate a strategy for SC based on individual SoC. The voltage-based control applied for each PEV, inside some virtual group of EVs, is based on priority levels. The control compares individual PEV Soc with the average one of its station group. The strategy uses hysteresis control to modify the station charging currents (I_{rc}), controlling the active charge power (P_{rc}) in this way. The model contains four virtual station groups with a certain number of stations connected, resulting from a random scenario generation.

The other sections of this article are divided as follows. Section II is a brief revision of the standard for charging mode. Section III showed the methodology of this work, the equipment used, the system for random scenario generation, and the SC strategy. Section IV presents a PHIL simulation case showing the problems of undervoltage and the SC strategy results. Furthermore, the last section is about the conclusions regarding the efficiency of the SC method and the impact of PEVs on the simulated grid.

II. RELATED STANDARDS

According to [15], the EV charging modes are defined mainly by a function of provided power, current/voltage range, and connection to the power supply. Charging mode 3, used in this work, is applied when an electric vehicle is permanently connected to a power supply system in alternating current with a dedicated socket and a control pilot that extends from the power supply to the EV in alternating current. Usually, the load of this mode is between 3.5/22 kW depending on current and voltage connection. This work uses a three phase mode 3 charging point connected to 220 V (V_{rc}) with a maximum current of 32 A achieving 12.2 kW.

Also, in the Brazilian context, the Paranaense Energy Company (COPEL) developed a technical standard [16] focused on how many parking spaces are intended for EV charging stations in public places such as shopping malls and supermarkets, defining 2% of all parking spaces.

III. METHODOLOGY

A. General Overview

Based on random scenarios, the current article proposed to analyze the impact caused by a different quantity of power demand for recharging EVs. The voltage profiles are analyzed to identify the undervoltage problem in a distribution system. This work used the Smart Grids laboratory at Electrical Energy Research Center (Cepel) which has a PHIL area test bench represented in (Figure 1) where the equipment trademarks are shown under the diagram. So, a modified version of the IEEE 34 Node benchmark is modeled, in the real-time simulator (RTS), to represent a distribution system with groups of stations, which the occupation is explained in the next chapter. This benchmark is based on a real system located in Arizona's state in the United States, having voltage rated 24.9 kV, two lightly loaded line regulators, one 4.16 kV unbalanced load, and shunt capacitors, which detailed parameters are described in [17]. The unbalanced load values per phase of (P [kW]; Q [kVar]) are: phase A (262; 133), phase B (240; 120), phase C (220; 114). Regarding the original benchmark data, this unbalanced loads were set to 85% of its nominal values, to represent a peak load hour.

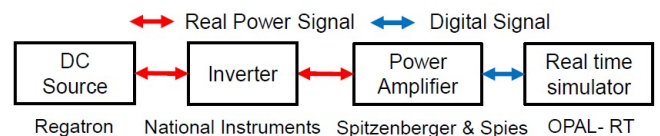


Fig. 1. Cepel's PHIL test bench schematic

In Figure 1 the DC-AC programmable inverter (PGINV), made by a National Instrument company, is used to emulate the onboard charger inside the EV, and it is connected to the virtual system of the IEEE 34 node through the power amplifier (PA). The inverter has a maximum power of 15 kW, is connected to a 380 V grid, and has an output setpoint of a maximum of 14 A. As mentioned, a PA connects the virtual system and the real world. This equipment transforms the digital references coming from RTS, per fiber optic connection (Aurora Protocol), into real voltage signals at its terminals where the inverter is connected, as can be viewed in Figure 1. The IA used during the simulations was the ideal transformer. The same logic is applied to close the loop by reading the currents signals transforming them into virtual signals, and sending them back to the RTS. On the DC side of the inverter, a DC source is connected to emulate the batteries inside the PEV.

Some gains were applied to simulate the scenarios as realistically as possible on a reduced scale because Cepel's programmable inverters have 15 kW. To obtain with this real inverter a power equivalent to mode 3 charging used on the virtual stations (connected in 220 V with 32 A, so a power of 12,2 kW), the gain of current needed, considering the closed loop factor of 0.6, was 38. The other gains used during the work can be observed in Table I, where the voltage gain represents the connection in 220 V on the simulation side, and the power relation represents 10 real stations emulated by Cepel's inverter.

The point of common coupling (PCC) of each group of

TABLE I
System Gains

Gain	Value
Current (Gi)	38
Voltage (Gv)	220/380 = 0.5789
Power relations	122 kW/15 kW = 8.13

virtual stations (ST2-5), the voltage meters, and the real station (ST1) emulated by Cepel's inverter can be founded in Figure 2. Also, the modeled benchmark has voltage meters (Colorful rectangles) placed at strategic points to generate the graphical results for this work.

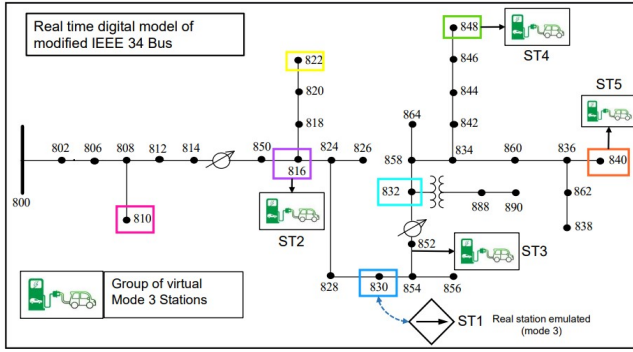


Fig. 2. IEEE34 Node simulated and PCC of the stations

The control strategy is applied based on individual PEV's SoC compared to a mean value of SoC inside its virtual group of stations, to avoid undervoltages problems, prioritizing the PEVs with the lower SoC. When the PEV gets priority 1, they charge at the maximum power (12.2 kW) permitted by used mode 3 [15]. However, the other PEVs with a SoC bigger than the mean have the I_{rc} reduced, charging at a lower level of P_{rc} (Priority 2 and 3). With this, the undervoltage problem is solved, while some PEVs charge at different power levels.

B. System for Random Scenarios Generation

Based on used charge mode 3, with a P_{rc} of 12.2 kW, the following definition is made: (i) the group of stations ST1 is real stations emulated by the PHIL test bench. (ii) the group of virtual stations ST2 – ST5 (Figure 2) was modeled inside RTS, connected in 220V. The occupation of these virtual stations is made using random scenarios, as depicted in (1) connecting 12 to 18 PEVs. Every time the simulation starts, it gives the number of PEVs (k) in each virtual station (n). Also, the SoC of each PEV, between 30 and 65%, is generated randomly using (2).

After these parameters are defined, a current of 32 A is applied, per PEV, to obtain the maximum possible charge power. The value adopted was considering the type 2 plugs and cables, which can support 22 kW and 32 A. Therefore, using the simulation PEVs with an equal battery capacity (Batcap) and having the SoC values generated by (2), it is possible to define how much energy will need in each of the groups of virtual stations using (3).

$$Cars_n = randi([12 \ 18], 4, 1) \quad (1)$$

$$SoCST_n = randi([30 \ 65], Cars_n, 1) \quad (2)$$

$$E_{rc} = Cars_n \cdot [Batcap - (SoCST_n \cdot Batcap)]. \quad (3)$$

C. Smart-Charging Strategy

Smart charging control starts when some voltage profile surpasses the lower limit of the defined band at 0.9 pu. For the upper limit, the strategy used the lowest value of the appropriate voltage section for the supply, according to Prodist (Brazilian standard) [18]. The value of this limit is approximately 0.918 pu or 2% above the band lower limit, being responsible for terminating the control when any voltage profile exceeds it. Therefore, with each PEV's SoC value inside the group of virtual stations defined, a priority classification to charge in maximum power is made. The flowchart from Figure 3 shows the adopted logic with field division. The analysis field represents the examination of voltage profiles and if the control is activated or not. The process field represents receiving data from random scenarios. The decision is to locate each PEV at some priority level, and the last field is to apply the new recharge current (I_{rc}).

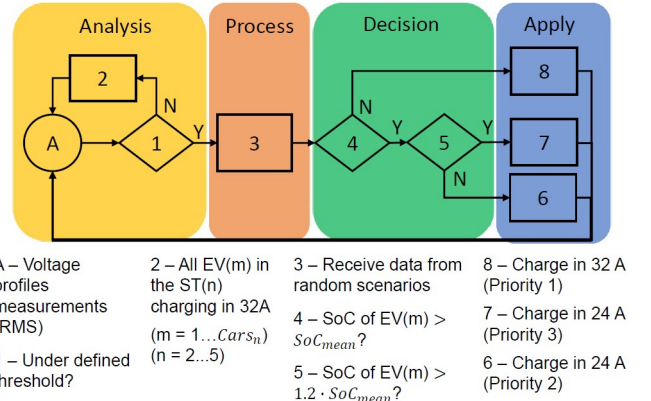


Fig. 3. Flowchart of Smart charging strategy

Charging the PEV with 32 A indicates that PEV's SoC is smaller than the mean value of SoC (SoC_{mean}) at that group of stations. If the PEV SoC is greater or 20% greater than SoC_{mean} the PEV will charge in priority 2 or 3, respectively, in 24 A with lower power. This value was chosen based on commercial charge stations that could select the nominal recharge current. During the simulation, the vehicles do not change to other priority levels maintaining the order created in the beginning. The time of recharge is not considered in the strategy defined by the authors because it was assumed that the PEV owner will accept a greater recharge time to receive a discount on the energy price for they contribute to guaranteeing the distribution power quality.

The P_{rc} value for each EV and the total station power P_{ret} is made by (5) and ,respectively.

$$P_{rc} = \sqrt{3} \cdot V_{rc} \cdot I_{rc} \quad (4)$$

$$P_{ret} = \sqrt{3} \cdot V_{rc} \cdot I_{rc} \cdot Cars_n. \quad (5)$$

D. Virtual Stations Configuration

The model of virtual stations can be observed in Figure 4. using Simulink's library. On the right top, it has three-phase connections with the benchmark IEEE34 Node in 24.9 kV. As presented, a step-down transformer is used to meet the desired charge voltage of 220 V. At the bottom of the figure, the active and reactive power control is shown, with the SC logic inside analyzing the variables in real-time. The power references are sent to the three-phase dynamic load. This block represents the group of virtual stations with PEVs connected. Inside the control block (Matlab Fcn), the SC strategy receives the data at the process field as shown in Figure 3 with the decrescent SoC priority order organized inside constant blocks Prio3/2/1. This block contains the number of PEVs and this will be multiplied by the value of I_{rc} constant block (I_charg_level), inside the Matlab Fcn, according to the priority classification made in the decision field. So, the I_{rc} values are applied at the last field of the flowchart shown in Figure 3, sending new P_{rc} values in this station to the three-phase dynamic load as a reference.

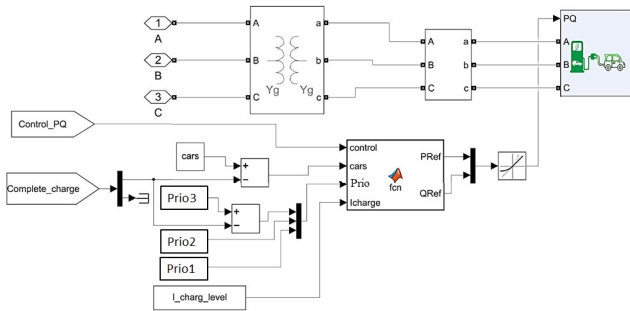


Fig. 4. Model of virtual stations

E. Real Stations Configuration

The next step is modeling the group of ten real stations emulated by Cepel's equipment, shown in, Figure 5. In this case, the programmable inverter works as the onboard converter inside the EV, and the DC source is used in the 4th power flow quadrant to emulate the EVs batteries. The PA is responsible to connect the inverter AC side to the virtual electrical system to close the loop at PHIL simulations.

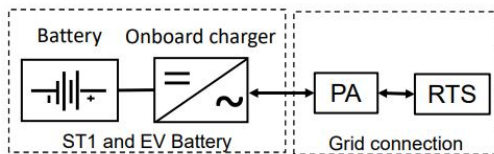


Fig. 5. Model of real stations

F. Programmable Inverter

Figure 6 presents a schematic of the programmable inverter's internal configuration. It divides into two main parts. The Active Front End (AFE) is responsible for converting AC voltages from the simulated grid into DC at DC intermediate bus. The other part is the Back End (BE), responsible for DC/DC conversion between the intermediate DC bus and the DC side, which is the DC source.

When the PGINV is used by the human-machine interface

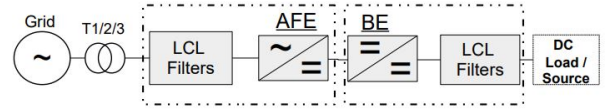


Fig. 6. Programmable inverter internal configuration diagram

(HMI), operating the AFE first is indispensable because the AFE is responsible for controlling the intermediate DC bus voltage. Only after this control has been made it is possible to adjust the BE. On BE side is where it is possible to control the current demanded by the PEV to charge the batteries. While this current increases, the undervoltage will appear in some simulated buses inside RTS, starting the SC strategy on the group of virtual stations (ST2 – 5).

IV. RESULTS

The simulated case is an example of peak hour load investigation. Therefore, by setting 85% of the load connected to the IEEE34 Node, it is possible to see the impact caused by the PEV connection by analyzing the voltage profiles. The first step is to identify the number of PEVs connected in each group of virtuals station (Figure 7). Moreover, a control variable named complete_charge can be observed in Figure 7. The value of the block will be modified, at the end of the simulation, to apply the variable EV_out, which represents a random number of PEVs that will be disconnected from the charge station, in order to emulate the decision of the PEV owner to stop recharging. By this, the number of PEVs connected to the grid decreases, reducing the power demand and ending the SC. The EV_out is obtained using (6), it uses the number of EVs in priority 3 as the maximum value because they represent the EVs with the greater SoC.

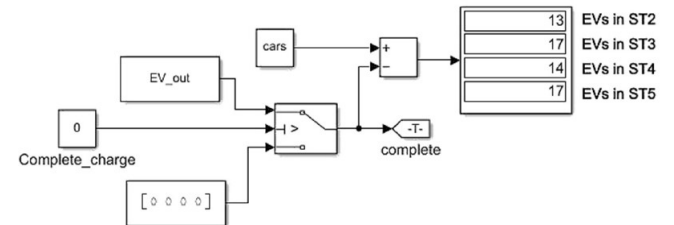


Fig. 7. EVs per group of virtual stations

$$EV_{out} = randi([1 \text{ Prio3}], 4, 1). \quad (6)$$

The second step is to observe the real currents, that came from PGINV to RTS, influencing the grid voltage profiles. The Figure 8 shows the real currents in the upper graphic and the voltage profiles, preserving the color relation with Figure 2, in the lower. The P_{rc} during this second step is the maximum (12.2 kW). In 0.24 seconds ten real stations (ST1) were inserted, at the same time, into the system, and the measured voltage profiles started to decrease. Besides that, at around 0.25 seconds the stations were completely connected and the voltage profile from PCC stayed under the undervoltage limit of 0.9 p.u. ($Lower^{Limit}$), characterizing a power quality problem for the grid operator.

Considering the geographic and load definitions of the current work, a PEV host capability of 71 was found. The

distribution is made according to Figure 7 (61 PEVS in ST2-5 and 10 PEVs in ST1) causing the problem of undervoltage. By varying the charge current I_{rc} at the group of virtual stations, the control of active charge power was done, avoiding the undervoltage occurrences, and increasing the voltage profile above $Lower^{Limit}$ around 0.26 seconds. Now the voltage profiles are above the $Lower^{Limit}$, however it still under the $Upper^{Limit}$, therefore the SC is maintained. If all voltage profiles were above this limit, maximum P_{rc} is delivered for the PEVs (12.2 kW), charging them in 32 A. The control logic occurs according to Figure 3 flowchart reducing some PEVs I_{rc} to 24 A. The P_{rc} on ST2 can be observed in Figure 9, where can be observed a power reduction from approximately 179 kW to 143 kW when 9 PEVs (Prio 2 and 3) are recharging at 24 A.

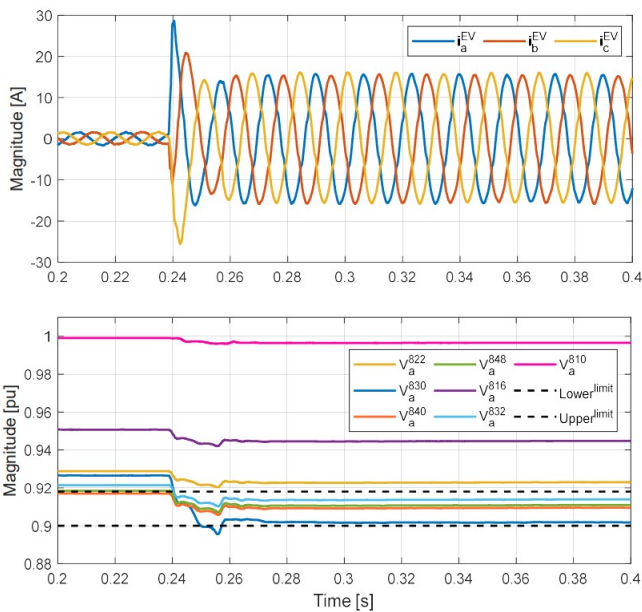


Fig. 8. Real currents and grid voltage profiles

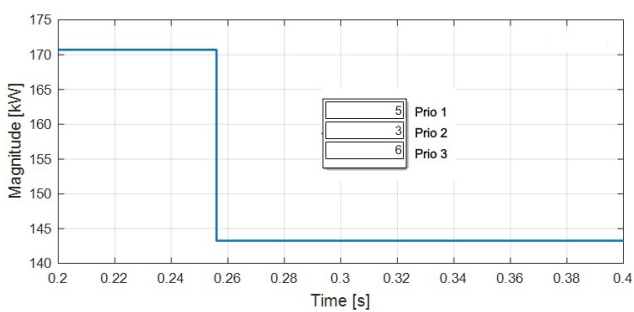


Fig. 9. Active power in ST2 considering the priority level control

After some time, the PEVs owner will disconnect the EV from the station. Therefore, using the control (complete_charge), PEVs are randomly disconnected from every group of virtual station. When they are disconnected, in Figure 10, the voltage profiles increase sufficiently to overreach the threshold $Upper^{Limit}$. With 5 PEVs disconnecting from ST2, the remaining 8 are charging with 32 A and a P_{rc} around 97 kW, as shown in Figure 11.

To understand the influence of the number of vehicles,

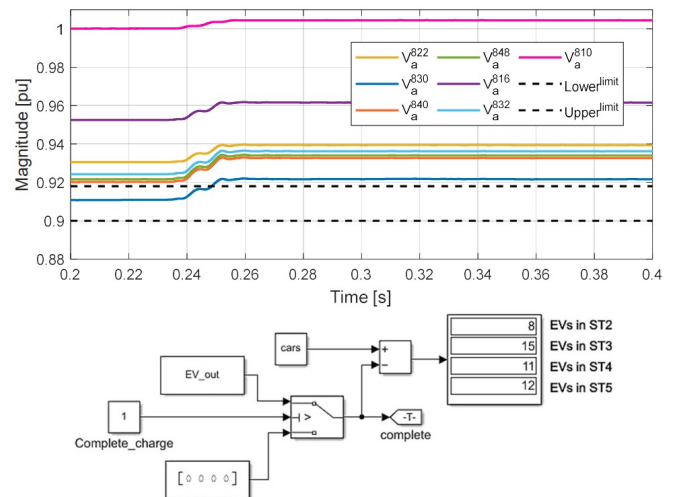


Fig. 10. Voltage profiles when PEVs randomly disconnected

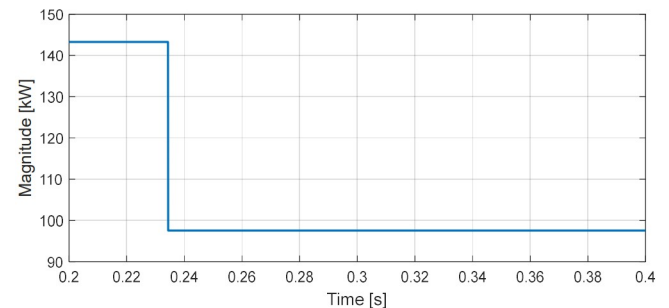


Fig. 11. Active power in ST2 after PEVs disconnect

another simulation was made, obtaining 74 EVs connected, distributed according to Figure 12 (64 in ST2-5 and 10 in ST1). As can be observed the undervoltage problem still occurring but in this case other voltage profiles different than the PCC goes under the $Lower^{Limit}$ around 0.2 seconds. These voltage profiles represent the end of the line voltage measurements which are expected to suffer more of voltage violations because of the distance from the generator source. Therefore, the control started and the voltage profile reached the $Upper^{Limit}$ but does not trespassed it (Figure 13), maintaining the PEVs in charge with a lower power.

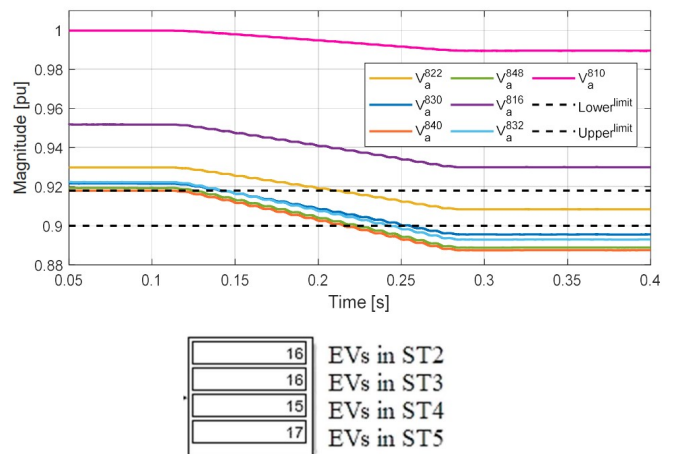


Fig. 12. Voltage profiles with 64 PEVs in ST2-5

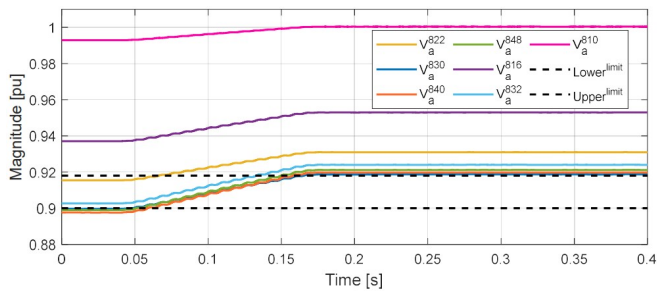


Fig. 13. Controlled voltage profiles

V. CONCLUSIONS

This paper demonstrated, with real-time simulations, the impact caused by plug-in electric vehicle (PEV) charging in distribution systems. The study presents that with the increase of active power required by PEVs for recharging, undervoltage problems could appear when approximately 71 PEVs are connected to the network. Two important factors to obtain this number are (i) the arrangement of the group of stations in the grid, as shown in Figure 2, and (ii) the ratio of loads connected (85%) to represent peak hours. Different conditions might change the number of PEVs connected. According to the results, the undervoltage problem is not limited to the station's point of common coupling, but rather a general where the magnitude of the problem of power quality can be observed in other buses, mainly at the end of the line when the number of PEV connected increases.

Therefore, smart-charging strategies are necessary to control and adapt the grid to this new power demand. The addressed control implemented in the group of virtual stations (ST2-5) was based on the vehicle's state of charge (SoC) analysis to define the charging priority when compared to the mean SoC of the local's group of stations. Thereby, the control adjusts the recharging current (I_{rc}) to a lower level (24 A) and, consequently, to a lower charging power (P_{rc}), keeping all PEVs connected to the grid without causing undervoltage problems. The I_{rc} of 24 A was chosen since this value is one of used by manufacturers of recharge stations. The control seeks to prioritize the PEV with lower SoC when compared to the mean, recharging them at the maximum possible power defined by the station and the recharge mode.

As this study only focuses on presenting a new smart charging strategy, based on individual SoC, to solve the undervoltage problem, the disconnection of PEVs with 100% SoC and new connections was not addressed here. However, the PEV owner decision on disconnecting the PEV from the station was made randomly. Besides that, the authors suggest, as future work, analyze the recharge time to ensure the performance of the control, vary the battery capacity values between the PEVs, applying other methods to linearly reduce I_{rc} , and changes in the parameters to define the priority levels.

ACKNOWLEDGEMENTS

The authors thank the Electrical Energy Research Center (Cepel), for providing Smart-Grids laboratory equipment for this work. The authors also thank the Foundation Carlos Chagas Filho Research Support of the State of Rio de Janeiro (FAPERJ) for the financial support, and their research partners

of Smart Grids Laboratory contributed support, time, and knowledge to make this work possible.

REFERENCES

- [1] International Energy Agency, "Global EV Outlook 2023", 2023, [Online], URL: <https://www.iea.org/reports/global-ev-outlook-2023>.
- [2] ABVE, "Eletrificados: novo recorde no semestre", 2023, [Online], URL: <http://www.abve.org.br/eletrificados-novo-recorde-no-semester/>.
- [3] T. Teoh, "Electric vehicle-charging strategies for Urban freight transport: concept and typology", *Transport Reviews*, vol. 42, pp. 157–180, Jul. 2022, doi:10.1080/01441647.2021.1950233.
- [4] Z. Jiang, L. Shalalfeh, M. J. Beshir, "Impact of electric vehicles on the IEEE 34 node distribution infrastructure", *International Journal of Smart Grid and Clean Energy*, Oct. 2014, doi:10.12720/sgce.3.4.417-424.
- [5] M. Schücking, P. Jochem, O. W. Wolf Fichtner, K. Stella, "Charging strategies for economic operations of electric vehicles in commercial applications", *Transportation Research Part D: Transport and Environment*, vol. 51, pp. 173–189, Mar. 2017, doi:10.1016/j.trd.2016.11.032.
- [6] N. Daina, A. Sivakumar, J. W. Polak, "Electric vehicle charging choices: Modelling and implications for smart charging services", *Transportation Research Part C: Emerging Technologies*, vol. 81, pp. 36–56, Aug. 2017, doi:10.1016/j.trc.2017.05.006.
- [7] S. I. Spencer, Z. Fu, E. Apostolaki-Iosifidou, T. E. Lipman, "Evaluating smart charging strategies using real-world data from optimized plugin electric vehicles", *Transportation Research Part D: Transport and Environment*, vol. 100, Nov. 2021, doi:10.1016/j.trd.2021.103023.
- [8] M. Brenna, F. Foiadelli, C. Leone, M. Longo, "Electric Vehicles Charging Technology Review and Optimal Size Estimation", *Journal of Electrical Engineering and Technology*, vol. 15, pp. 2539–2552, Nov. 2020, doi:10.1007/s42835-020-00547-x.
- [9] B. Canizes, J. Soares, A. Costa, T. Pinto, F. Lezama, P. Novais, Z. Vale, "Electric vehicles' user charging behaviour simulator for a smart city", *Energies*, vol. 12, Apr. 2019, doi:10.3390/en12081470.
- [10] J. A. Lopes, F. Soares, P. Almeida, M. da Silva, "Smart Charging Strategies for Electric Vehicles: Enhancing Grid Performance and Maximizing the Use of Variable Renewable Energy Resources", in *EVS24 International Battery, Hybrid and Fuel Cell Electric Vehicle*, Stavanger, Norway, Dec. 2009.
- [11] S. Faddel, A. T. Al-Awami, O. A. Mohammed, "Charge control and operation of electric vehicles in power grids: A review", *Energies*, vol. 11, Apr. 2018, doi:10.3390/en11040701.
- [12] F. Lehfuss, G. Lauss, C. Seitzl, F. Leimgruber, M. Noehrer, T. I. Strasser, "Coupling of Real-Time and Co-Simulation for the Evaluation of the Large Scale Integration of Electric Vehicles into Intelligent Power

Systems”, in *IEEE Vehicle Power and Propulsion Conference (VPPC)*, pp. 1–5, 2017, doi:10.1109/VPPC.2017.8331020.

- [13] D. F. Pereira, F. D. C. Lopes, E. H. Watanabe, “Nonlinear Model Predictive Control for the Energy Management of Fuel Cell Hybrid Electric Vehicles in Real Time”, *IEEE Transactions on Industrial Electronics*, vol. 68, pp. 3213–3223, Apr. 2021, doi: 10.1109/TIE.2020.2979528.
- [14] G. F. Lauss, M. O. Faruque, K. Schoder, C. Dufour, A. Viehweider, J. Langston, “Characteristics and design of power hardware-in-the-loop simulations for electrical power systems”, *IEEE Transactions on Industrial Electronics*, vol. 63, pp. 406–417, Jan. 2016, doi:10.1109/TIE.2015.2464308.
- [15] ABNT, “Electric vehicle conductive charging system Part-1: General requirements”, 2017, [Online], URL: www.abnt.org.br.
- [16] COPEL, “Norma Técnica COPEL-NTC Fornecimento De Energia Estações De Recarga De Veículo Elétrico NTC 902210”, 2019, [Online], URL: <https://www.copel.com/site/fornecedores-e-parceiros/pesquisa-de-normas-tecnicas/>.
- [17] IEEE, “1992 – Test Feeder Cases”, , 2017, URL: <https://cmte.ieee.org/pes-testfeeders/resources/>.
- [18] ANEEL, “ANEXO VIII da Resolução Normativa nº 956, Procedimentos de distribuição de energia elétrica no sistema elétrico nacional - PRODIST”, 2021, [Online], URL: https://www2.aneel.gov.br/cedoc/aren2021956_2_7.pdf.

BIOGRAPHIES

Frederico Haasis obtained a Bachelor’s degree in Electrical Engineering from the University Center of Volta Redonda in 2021. He is currently a Master’s student in the Graduate Program in Electrical and Telecommunications Engineering (PPGEET) at the Fluminense Federal University (UFF) and a master’s scholarship holder at the Smart Grids laboratory

of the Electric Energy Research Center (Cepel), working in the field of distributed generation, electric vehicles, and smart grids.

Oscar Solano obtained the title of electrical engineer (2011) from the Universidad Industrial de Santander, and the titles of master (2014) and doctor (2019) in Electrical Engineering from the Federal University of Rio de Janeiro (UFRJ), both in the field of Power Electronics. Since 2014 he has been a researcher at the Electric Energy Research Center (Cepel). Since 2022 he is the technical manager of the Smart Grids Laboratory. His areas of expertise are real-time digital simulation, hardware-in-the-loop tests, experimental compliance tests in electric power converters, simulation of power electronic converters, hybrid microgrids, and pluggable electric vehicles.

Bruno França received the B.Sc., M.Sc., and D.Sc. degrees in electrical engineering from the Federal University of Rio de Janeiro, Rio de Janeiro, Brazil, in 2009, 2012, and 2016, respectively. Since 2017, he has been an Associate Professor with the Department of Electrical Engineering, Fluminense Federal University (UFF), Rio de Janeiro. He is ahead of the Laboratory for Novel & Interdisciplinary Technologies in Electrical Engineering (NITEE), a Research Group founded, in 2018, of the Postgraduate Program in electrical and telecommunications engineering. His research interests include power electronics, distributed generation, microgrids and smart grids, power quality issues, renewable and energy storage systems, HVDC transmission, flexible AC transmission systems, and active filters.

Daniel Dias received a bachelor’s degree in physics and electrical engineering from the Federal University of Rio de Janeiro (UFRJ), in 2003 and 2011, respectively. He received a Master’s degree in physics from Federal Fluminense Federal University (UFF) and a Doctor’s degree from UFRJ in 2009. Currently, he holds an associate professor position at UFF, in the Department of Electrical Engineering. His research interest has been in electric vehicles, batteries and the study of renewable energy systems.